New chaotic system, a compromise between structural simplicity and the complexity of its dynamic behaviour

FRIDJAT Mohammed Elkamel [1], SADAOUI Djaouida [2]

[1] Faculty of Technology, Department of electronics, LEA Laboratory, University of Batna 2 (Mostefa Ben Boulaid), Batna, Algeria, Email (m.fridjat@univ-batna2.dz)
[2] Department of Science and Technology, LEA Laboratory University of Batna 2 (Mostefa Ben Boulaid), Batna, Algeria, Email (d.sadaoui@univ-batna2.dz)

Received: 12/07/2024; Accepted: 09/12/2024

Abstract:

Our paper focuses on the discovery and analysis of a recently identified three-dimensional chaotic model. This research presents a remarkable system characterised by its ease of implementation, but which exhibits a more complex dynamic behaviour, exceeding that of many similar chaotic systems. By unravelling the underlying mechanisms of this system through the analysis of eigenvalues, bifurcation diagrams and Lyapunov exponents, its chaotic behaviour is verified by building an electronic circuit. The experimental behaviour is in agreement with the numerical studies. This paper paves the way for further exploitation of the unique interplay between simplicity and complexity in chaotic systems, promising applications in various scientific disciplines.

Keywords: Nonlinear dynamics; Chaos; Strange attractor; Bifurcation; Lyapunov exponents; Poincare section.

1. INTRODUCTION

In the constantly evolving field of dynamical systems theory, the search for new chaotic systems is ongoing. These systems, often characterised by their complex dynamical behaviour, play an important role in various fields such as physics [1,2], engineering [3,4], biology [5] and finance [6,7]. This article explores the delicate balance between the structural simplicity of a recently discovered chaotic system and the fascinating complexity of its dynamic behaviour. In the field of chaos theory, the Lorenz system is an emblematic example of deterministic chaos. The Lorenz equations, formulated by Edward Lorenz in 1963 [8], provide a vivid illustration of how the simplest mathematical systems can exhibit complex and unpredictable behaviour. In this article we look at the implications of this compromise, highlighting its relevance, which opens the way to practical applications in areas such as image encryption [9-14], secure communication [15-17] and the modelling of complex systems [18]. The chaotic system in question is striking for its structural simplicity. Unlike many chaotic systems with convoluted equations and complex geometries, they often require significant computing resources and specialist expertise, making them difficult for many researchers to interpret. Our analysis will begin in Section 2 with an in-depth examination of the equations and parameters of the system, revealing the mathematical essence underlying its chaotic nature. Section 3 deals with the structure of the system's attractors, revealing the complex geometries that emerge from its dynamics. Along the way, we will perform analyses of the properties of the proposed system in terms of the Poincare map, Lyapunov exponent spectra, bifurcation diagrams, basin of attraction, to identify critical points where chaos emerges from order, allowing us to assess the sensitivity of the system to initial conditions and its potential and to understand how the system can be controlled and manipulated. Here, all simulations are carried out using the ode45 solver in the MATLAB simulation environment. The results of this section imply the existence of chaotic behaviour for certain parameter values. The chaotic behaviour is then confirmed by the implementation of the electronic circuit in section 4, which corresponds to the numerical results. Finally, the conclusions of this work are presented in section 5, with an outlook on future work.

2. FORMULATION AND DESCRIPTION OF THE MODEL

The proposed system is a unique three-dimensional system of autonomous ordinary differential equations (ODEs) consisting of two non-linear terms.

The equations are as follows.

$$\begin{cases} \dot{x} = -ax + y + z \\ \dot{y} = -cxz - y \\ \dot{z} = xy - b \end{cases} \tag{1}$$

where a, b, c are constants ($a = 3.3, b = 5, c = 19.001$) and x, y, z are the state variables of the system. The terms involving products of variables (xy, xz) contribute to the complexity and unpredictability of the system dynamics, leading to chaotic trajectories in phase space.
The parameter b, which is equal to 5, introduces a shift in the baseline, influencing the stability of z, and its variation contributes to the dynamic behaviour of the system.

3. ANALYSIS OF THE PROPOSED SYSTEM

Chaotic performance can be evaluated using various techniques such as equilibria and stability, Lyapunov exponents, Kaplan-Yorke dimension and bifurcation.

A. Equilibrium and stability analysis

The system has three equilibria where the derivatives of all variables are zero $\dot{x} = 0;\ \dot{y} = 0;\ \dot{z} = 0$, which are respectively described as follows:

$$E_1^*(-1.25643, -3.97952, -1.66699);$$

$$E_2^*(1.20370, 4.15384, -0.18163); \tag{2}$$
$$E_3^*(0.05272, 94.83068, -94.656704)$$

The stability of the equilibrium points is assessed by calculating the Jacobian matrix of the system (1) at equilibria E^* is as follows:

$$J_E^* = \begin{pmatrix} -3.3 & 1 & 1 \\ -19.001z & -1 & -19.001x \\ y & x & 0 \end{pmatrix} \tag{3}$$

and the corresponding eigenvalues are (obtained using Matlab).

$$\begin{aligned} \lambda(E_1^*) &\to \lambda_1 = -7.6402, \ \lambda_{2,3} = 1.67015 \pm 3227i \\ \lambda(E_2^*) &\to \lambda_1 = -5.6955, \ \lambda_{2,3} = 0.69775 \pm 5395i \\ \lambda(E_3^*) &\to \lambda_1 = -45.6541, \ \lambda_2 = 41.4040, \lambda_3 = -0.0500 \end{aligned} \tag{4}$$

So, for the equilibrium points E_1^* and E_2^* we can deduce that the system, despite its instability, may exhibit oscillatory or spiral behaviour rather than purely divergent behaviour. And for E_3^* the system may exhibit unstable or chaotic behaviour.

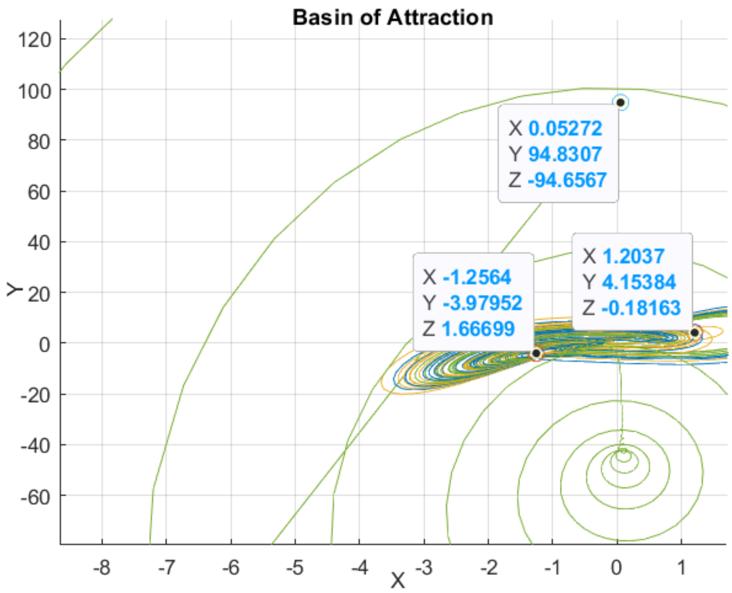

Fig. 1: Equilibrium points.

The eigenvalues provided indicate a mixed stability profile for the chaotic system. The equilibrium point associated with these eigenvalues is characterised by a combination of stable, unstable and potentially oscillatory behaviour. This complexity is typical of chaotic systems, where small perturbations can lead to divergent and complex trajectories over time. The detailed dynamics of the system can be further explored through numerical simulations and sensitivity analyses, given the non-linearities inherent in chaotic systems. Further analysis would be required to fully characterise the behaviour of the system, particularly in the presence of both stable and unstable eigenvalues.

B. Dissipative

The dissipativity or rate of contraction of the hypervolume of the phase space [19] of system (1) can be examined by calculating ∇V which is given by the Lie derivative:

$$\nabla V = \frac{\partial \dot{x}}{x} + \frac{\partial \dot{y}}{y} + \frac{\partial \dot{z}}{z} = -a - 1 = -4.3 < 0 \tag{5}$$

The system (5) is dissipative if the parameter $a > -1$. It can therefore generate chaotic behaviour. Based on the system parameters, we obtain $\nabla V = -4.3 < 0$, so the system is dissipative.

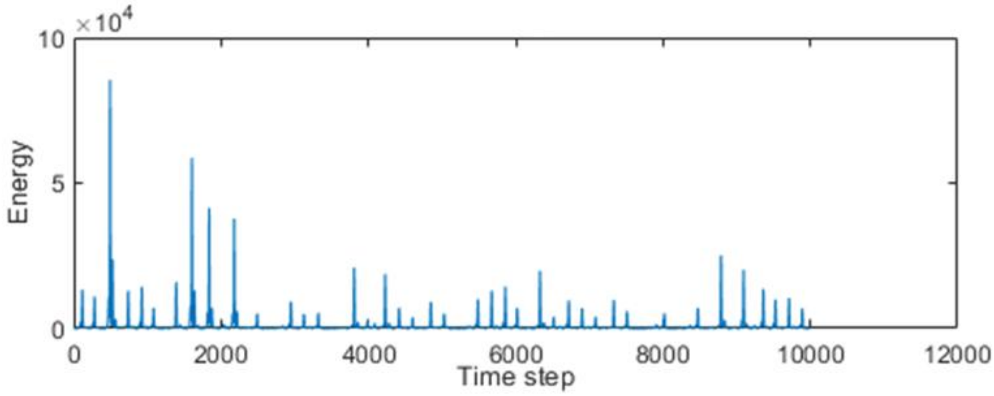

Fig. 2: Power spectrum.

And also..,

$$\frac{dV}{dt} = e^{(-a-1)} = 0.01356 \tag{6}$$

then the volume of the attractor decreases by a factor of 0.01356.

C. Numerical study

We present a detailed study of the dynamic behaviour of system (1) in numerical form. We have analysed the non-linear characteristics of the proposed system in terms of the Poincaré map, Lyapunov exponent spectra, bifurcation diagrams, phase diagram, basin of attraction and complexity, which gives us a clearer view of the characteristics studied.

D. Routes to chaos

By parameterising c and keeping a and b fixed, the system (1) exhibits different periodic and chaotic attractors. This is also shown by the bifurcation diagram in Fig.7.(b). Thus, this system generates the following shapes:

- If $0.1 \leq c \leq 3.25$, a limit cycle described in Fig.3.(a) is obtained.
- If $3.26 < c < 4.2$, we obtain a periodic orbit around the equilibrium point E_1^* described by Fig.3.(c).
- If $4.3 \leq c \leq 7.4$, a doubling of the period is described in Fig.3.(e).
- If $7.5 < c \leq 8.7$, a pseudo-periodic cycle is obtained, as illustrated in Fig.3.(b).
- If $8.71 < c \leq 16.8$, another periodic orbit is obtained around the two equilibrium points E_1^* and E_2^* by Fig.3.(d) with low chaos.
- If $16.9 < c \leq 19.001$, a chaotic attractor is formed with strong chaos, as shown in Fig.3.(f).

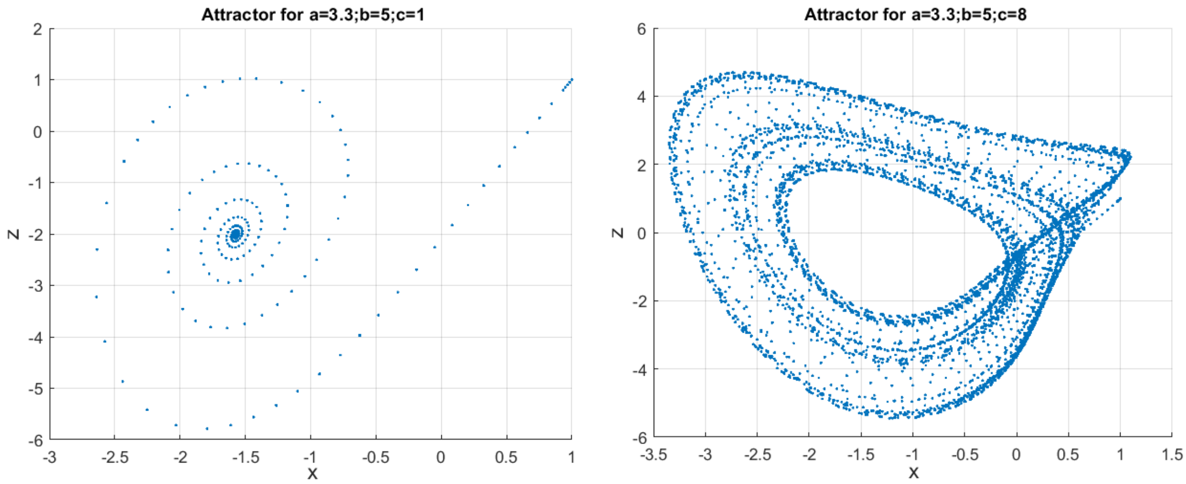

(a) (b)

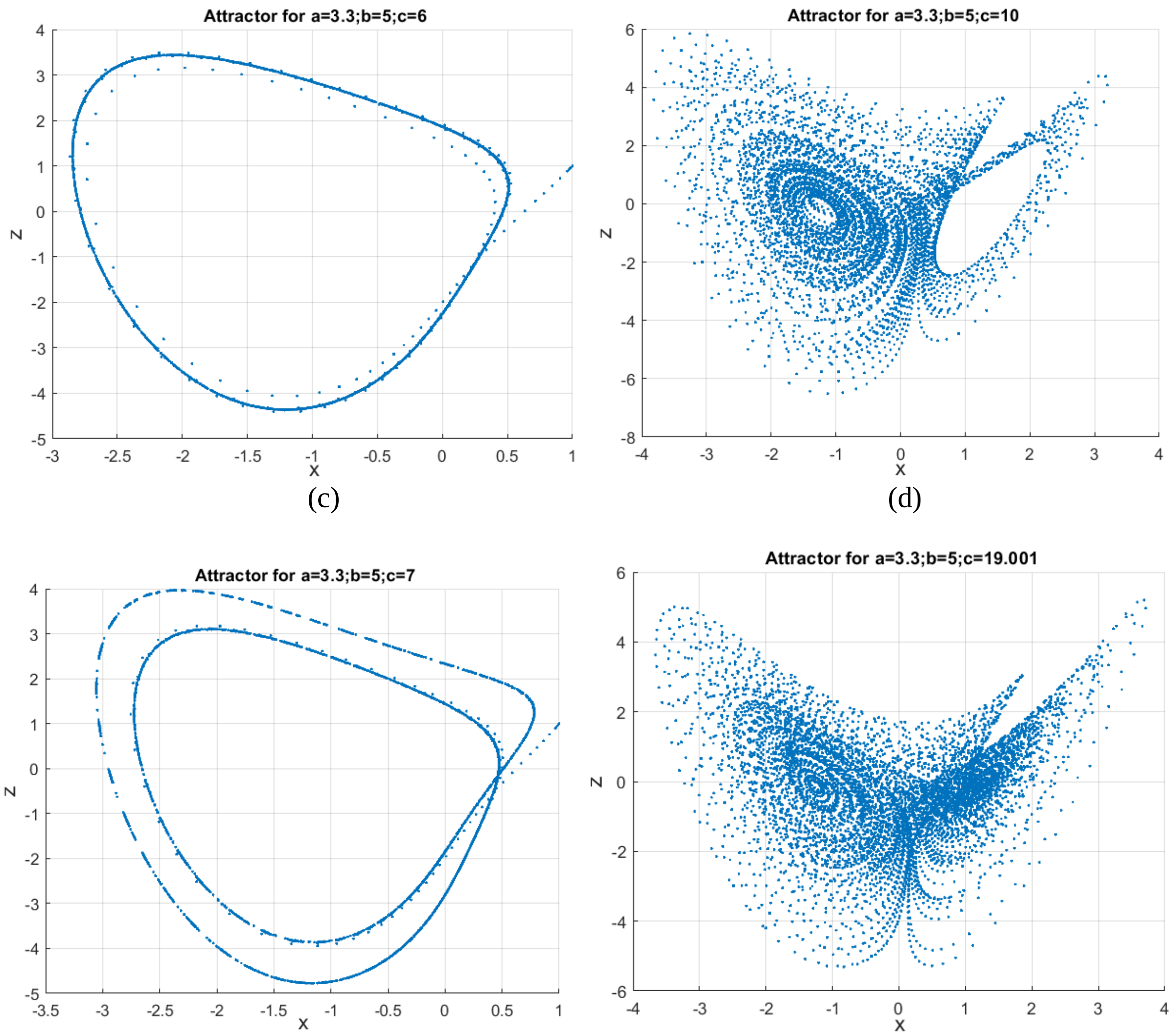

(c) (d) (e) (f)

Fig. 3: Fixing a = 3.3, b = 5, and initial values [1, 1, 1], the shape of the attractors changes with increasing parameter $c \in (1, 19.001)$.

Our results show that the system exhibits a series of complex and chaotic behaviours, including multiple attractors, periodic orbits and strange attractors.

E. The system's strange attractor and speed of travel

In a strange attractor, phase trajectories can travel through space in complex and unpredictable ways. Their speed of travel [20-22] varies considerably depending on their position within the attractor and the initial conditions of the system, which makes it difficult to define precisely.

The graph in Fig. 5 effectively illustrates the dynamic behaviour of the chaotic system, highlighting areas of stability and rapid change by colour-coding the speed of movement. The dense blue regions suggest areas where the velocity of the system is low and where it spends more time, which could indicate stable regions or local attractors within the chaotic system. The red and yellow regions indicate areas where the speed of the system is higher, showing rapid transitions between different states or attractor regions.

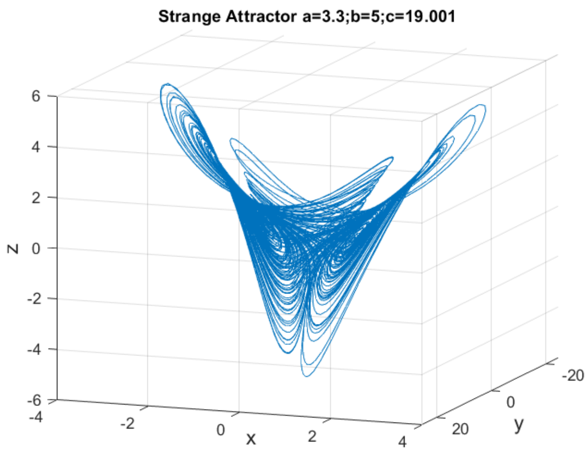

Fig. 4: Strange attractor for a = 3.3; b = 5 and c = 19.001, extreme chaos.

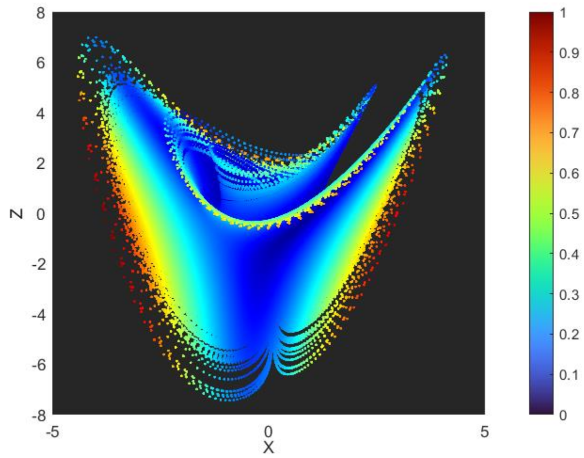

Fig. 5: Phase trajectory of the system for c = 19.001 and (a = 3.3 and b = 5), colours indicate the speed of travel.

F. Basin of attraction

Analysing the basin of attraction of a chaotic system involves exploring the initial conditions and understanding where the trajectories converge in phase space.

1) *By figure.6.(a):* This graph shows that E_1^*, shown in blue, and E_2^*, in red, seem to dominate a large part of the plane, which can be interpreted as a greater robustness of these equilibria to variations in initial conditions. Whereas E_3^* has a very restricted basin of attraction where complex transitions (in yellow) are observed between E_1^* and E_2^*, indicating sensitivity to initial conditions in these regions.

2) *By figure.6.(b):* The coloured lines represent different trajectories of the system starting from different initial conditions. The trajectories converge towards a particular region of phase space, known as a strange attractor, characteristic of chaotic systems.

3) *By figure.6.(c):* Although the initial condition is far from the attractor, the trajectory shows oscillations and complex loops before converging towards the attractor. that the system eventually converges towards the attractor. This illustrates the robustness of the attractor in the chaotic system, attracting trajectories even from distant initial conditions.

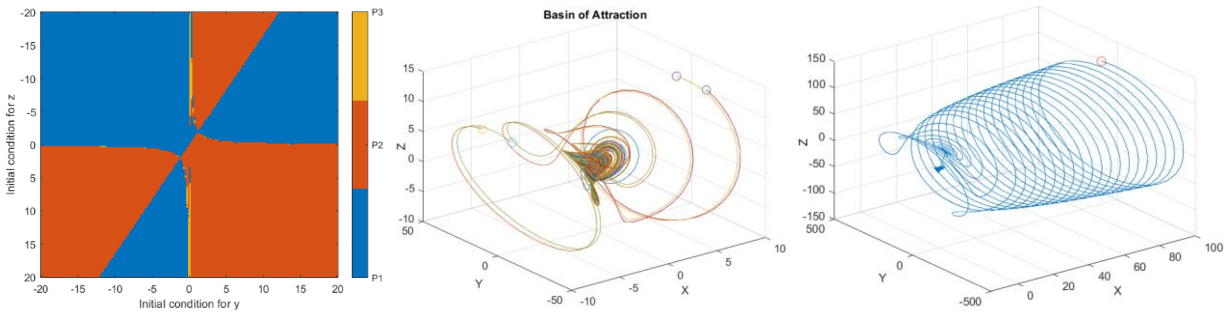

(a) (b) (c)

Fig. 6: Basin of attraction: (a): distribution of initial conditions in the space of variables (y, z) and their convergence towards one of the three equilibrium points E_1^*, E_2^*, or E_3^* (b): for different initial values: [0 0 0]; [10 10 10]; [-10 -10 10]; [10 -10 10]; [-10 10 10], (c): for initial values: [0 0 100].

G. Bifurcation, Lyapunov exponent and Dimension of Kaplan Yorke

To verify that system (1) is chaotic, the three Lyapunov exponents shown in Fig.7.(a) and calculated by Wolf's algorithm [23] are expressed as follows: Specific observations include the presence of periodic orbits, the appearance of bifurcation points indicating qualitative changes and the unveiling of chaotic regimes. The bifurcation diagram in Fig.7. (b) can be used to predict the response of the system to variations in parameter c, providing an overview of the system's behaviour and helping to identify the key transitions and critical values that govern its dynamics.

In summary, Lyapunov exponents give a nuanced picture of the three-dimensional chaotic system. The positive exponent λ_1 indicates chaotic behaviour and emphasises the unpredictability of the system. The quasi-neutral exponent λ_2 indicates a less dynamic direction, while the negative exponent λ_3 indicates stability and convergence. Together, these exponents provide an overview of the complex interplay between chaos and stability within the system, guiding in predicting its behaviour and making informed decisions in various scientific and engineering applications.

The Kaplan-Yorke dimension [24,25] is a measure of the fractal dimensionality of the system, reflecting the complex geometry of its attractors. In this case, $D_{KY} = 2.16$ suggests a non-integer fractional dimension. This fractional dimensionality is a characteristic of chaotic systems, indicating a complex, self-repetitive structure that does not conform to traditional integer dimensions.

Various systems from the literature are used in this analysis, as well as some special cases that cover a range of dimension $2 < D_{KY} < 3$. [26]

To illustrate the complexity of system (1), a comparison is made between the Kaplan-Yorke dimension and the largest Lyapunov exponent (LE) of the proposed chaotic system and those of well-known chaotic systems. As shown in Table 1, the proposed system has a larger Kaplan-Yorke dimension and a larger LE than most other systems, making it a more complex system.

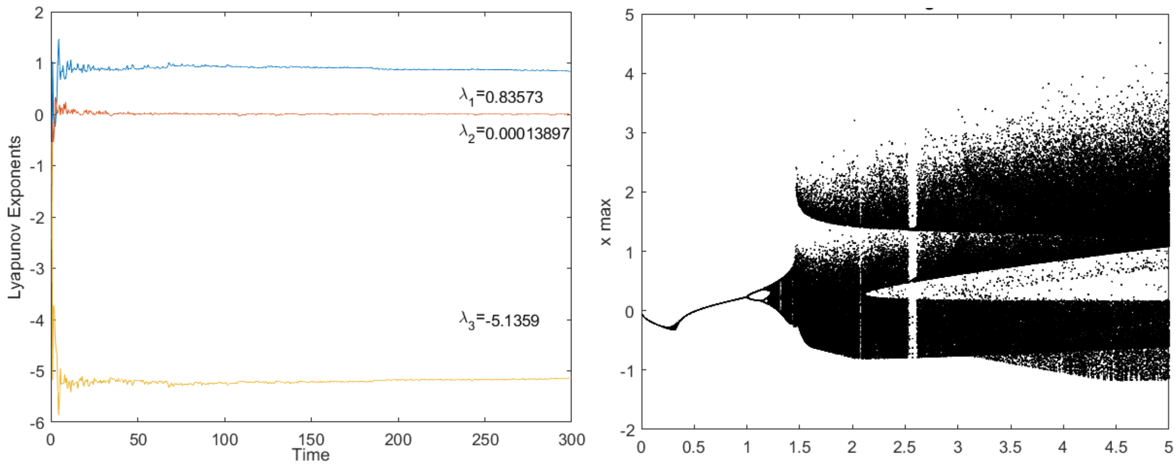

(a) (b)

Fig. 7: The Lyapunov exponent spectra and bifurcation diagrams of the system (1): (a) Lyapunov exponent spectra for $c \in (0, 40)$; (b) bifurcation diagram for $b \in (0, 5)$.

H. Poincare section

Poincare sections [27] are used to study the behaviour of dynamical systems by providing a lower-dimensional cut-out in the phase space of the system, enabling the structure of the system's trajectories to be visualised.

- Graph (a) shows simple, possibly periodic behaviour.
- Graph (b) represents a periodic movement with a single closed orbit.
- Graph (c) shows a transition to more complex dynamics.
- Graph (d) shows chaotic behaviour with a scattered distribution of points.

The Poincare sections in Fig.8. show the transition from simple periodic behaviour to chaos as the parameter c varies, demonstrating that the dynamics of the system becomes increasingly complex.

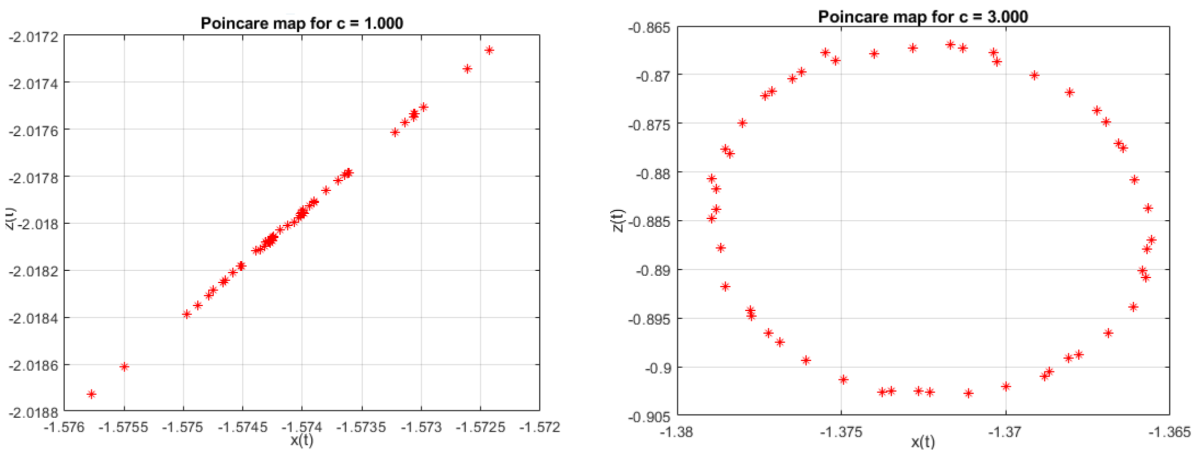

(a) (b)

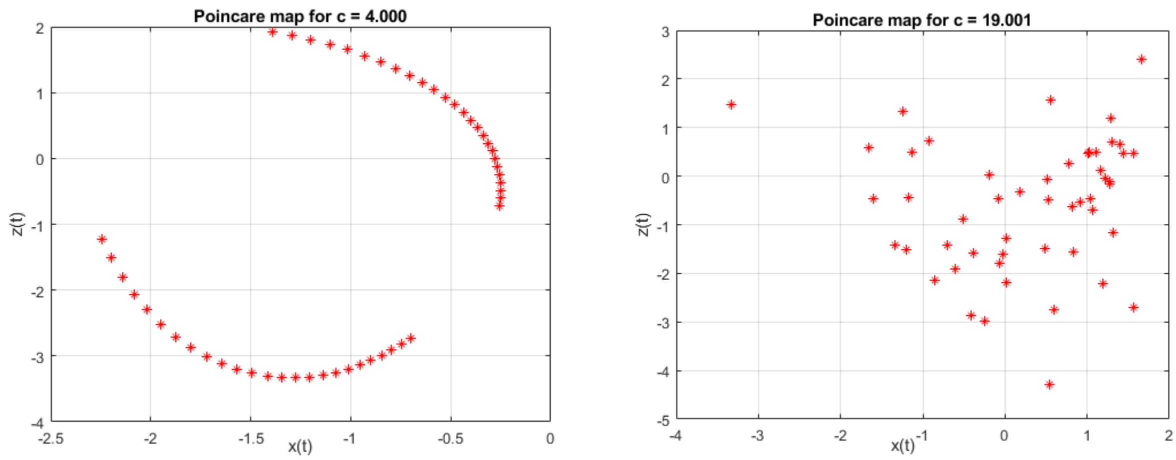

(c) (d)

Fig. 8: Poincare sections.

TABLE I: Comparison between the topology of the proposed system and similar simple 3D chaotic systems.

No	System	No of Nonlinear term	Maximum Lyapunov exponents	Maximum Kaplan York
01	Lorenz system [8]	2	$\lambda_{max} \approx 0.9056$	2.06
02	Rossler system [28]	1	$\lambda_{max} \approx 0.071$	2.01
03	Chen system [29]	2	$\lambda_{max} \approx 2.0$	2.27
04	Lu system [30]	2	$\lambda_{max} \approx 1.5$	2.14
05	Chua system [31]	1	$\lambda_{max} \approx 0.465$	2.03
06	Sprott system [32]	2	$\lambda_{max} \approx 0.231$	2.12
07	Halvorsen system [33]	2	$\lambda_{max} \approx 0.084$	2.06
08	Thomas system [34]	3	$\lambda_{max} \approx 0.076$	2.05
09	Newton-Leipnik system [35]	2	$\lambda_{max} \approx 0.129$	2.08
10	Proposed system	2	$\lambda_{max} \approx 0.83573$	2.16

I. Sensitivity to initial conditions and path to chaos

The most visible signature of a chaotic system is its sensitivity to initial conditions. We have simulated the dynamic behaviour of the system (1) starting from two neighbouring initial conditions (with a small variation in the coordinates). Fig.9 shows the dynamic behaviour of the state variables (x, y, z) and their errors starting from two initial conditions $(1, 1, 0)$ and $(1, 1, 0.001)$. We have deduced that the two trajectories exhibited by the system (1) for each variable are initially identical but become completely different after a certain time.

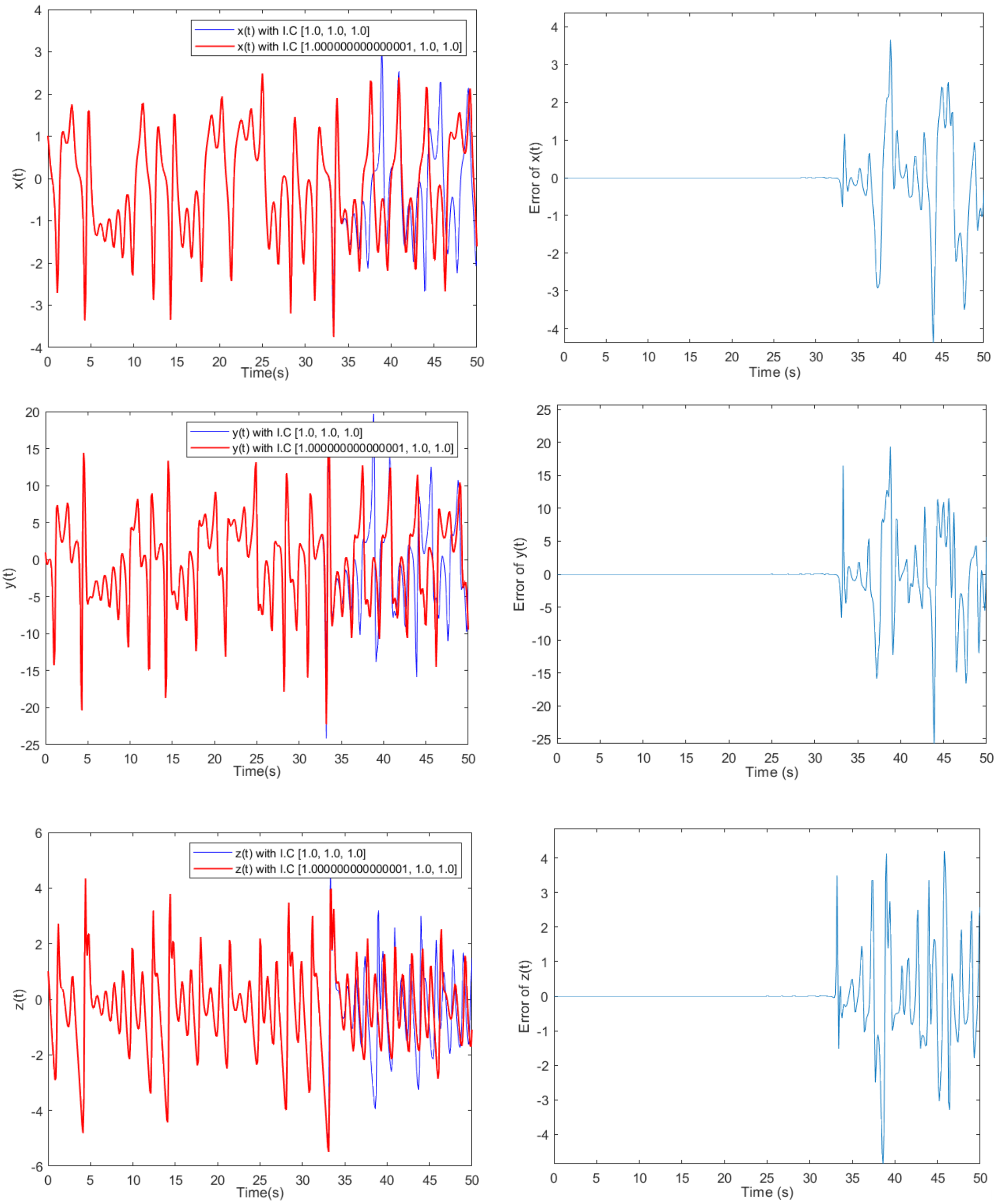

Fig. 9: Sensitivity to initial conditions ((1, 1, 1) and (1+ 10^{-15}, 1, 1)) of system (1): trajectories and errors of state variables x; y and z.

4. EXPERIMENTAL STUDY

The aim of this section is to design and implement a suitable analogue simulator for analysing the mathematical model defined by system (1). To this end, a schematic of the system (1) is proposed in Figure 10, designed by Multisim. This circuit consists of three channels, each of which implements one of the three variables in the model. The AD633JN [36] versions of Analog devices voltage multipliers are used to implement the non-linear terms of the mathematical model, and Operational amplifiers (type TL082 or TL084) [37] for addition and integration. It is also important to rescale the model by a factor for X, Y, Z in order to avoid saturation of the output signals of the operational amplifiers. The rescaled system reads as follows:

$$\begin{cases} \dfrac{dX}{dt} = \dfrac{1}{R_1C_1}X - \dfrac{1}{R_2C_1}Y - \dfrac{1}{R_3C_1}Z \\ \dfrac{dY}{dt} = \dfrac{1}{10R_4C_2}XZ + \dfrac{1}{R_5C_2}Y \\ \dfrac{dZ}{dt} = -\dfrac{1}{10R_6C_3}XY + \dfrac{1}{R_7C_3}v^+ \end{cases} \tag{7}$$

The system gives maximum chaos at: $a = 3.3$, $b = 5$ and $c = 19.001$, which correspond to the circuit values $C1 = C2 = C3 = 1nF$, $R1 = 303K\Omega$, $R2 = R3 = R5 = 1M\Omega$, $R4 = 5.2628K\Omega$, $R6 = R8 = R9 = R9 = R10 = R11 = 10K\Omega$. The capacitor values are chosen so that the signal frequency can be displayed on an oscilloscope. The resistors $R1$, $R4$ and the voltage $V1 = v+$ are adjusted to modify the parameters a, b and c in order to test the real-time dynamic behaviour of the system.

The results obtained by Multisim are shown in Figure 11, while the oscilloscope plots of the real circuit shown in the photo in Figure 13 are shown in Figure 12. Comparison of these results reveals good qualitative agreement. Since then, electronic circuits have been frequently used to study the existence and various properties of chaos [38-42].

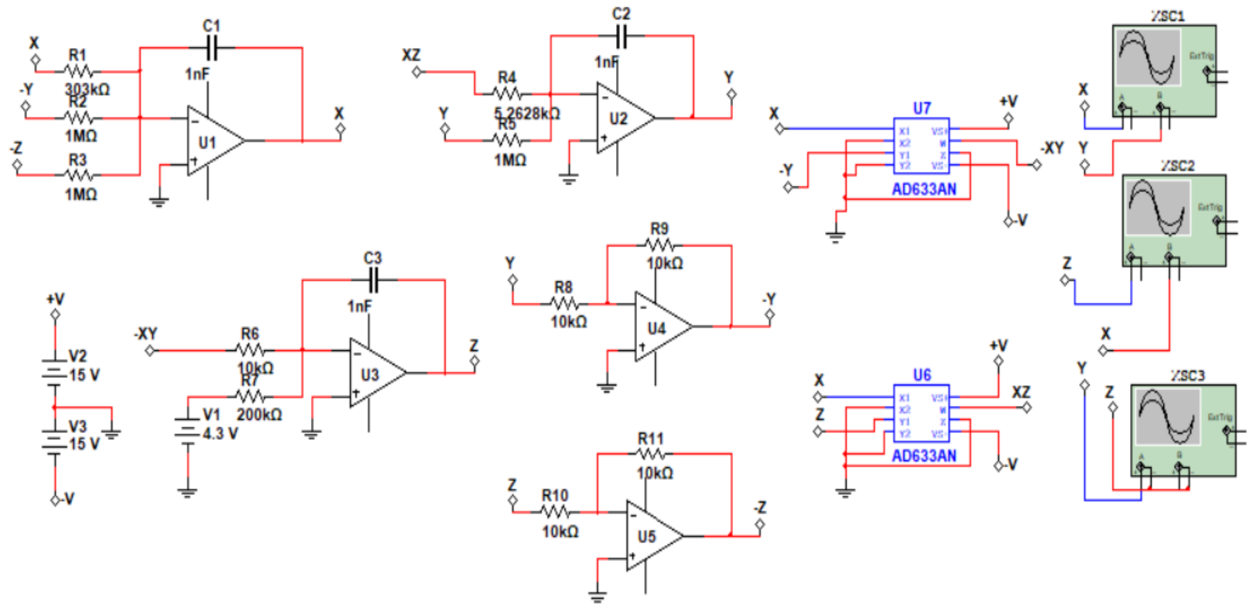

Fig. 10: Circuit schematic diagram of the system (1).

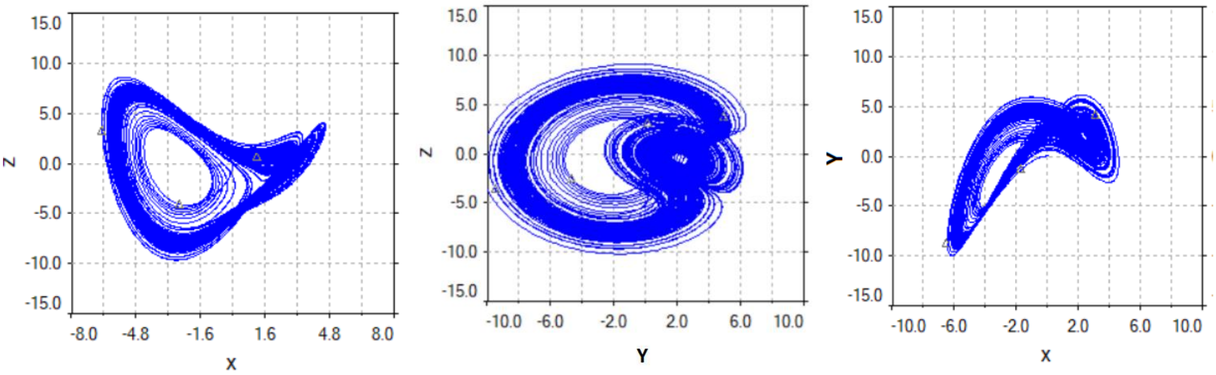

Fig. 11: State diagrams of the chaotic system with a = -3.3*,* b = -19.001 and c = 5 with Multisim.

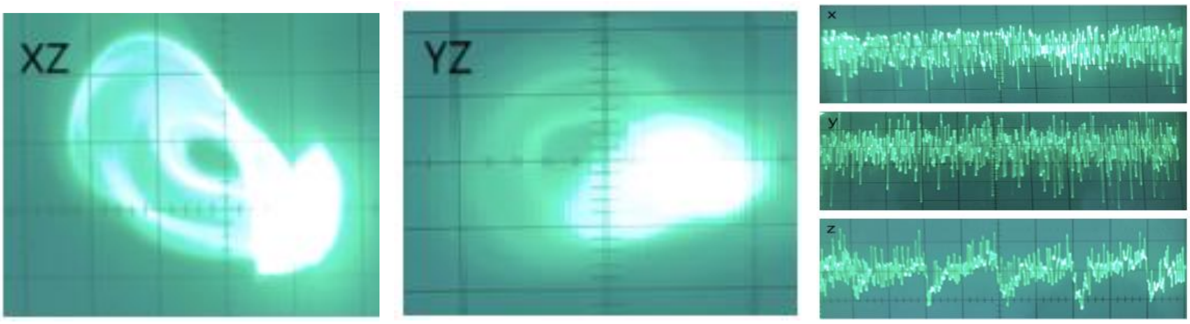

Fig. 12: Visualisation of the state diagrams of the chaotic system XZ, YZ and the random aspects of the state variables X, Y and Z as a function of time with a = -3.3*,* b = -19.001 and c = 5 on an oscilloscope.

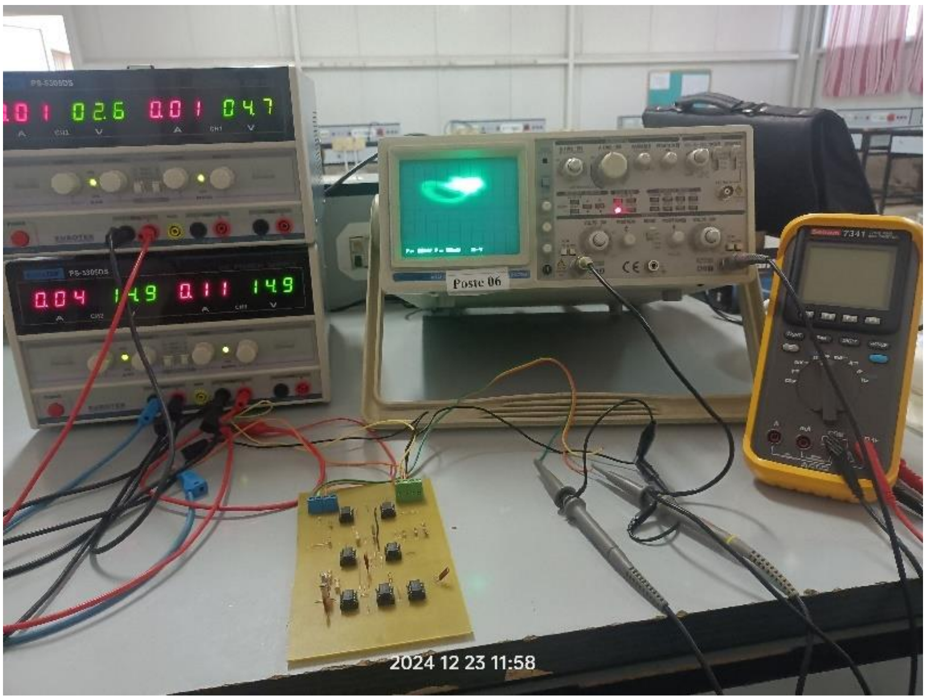

Fig. 13: Experimental implementation of the proposed system

5. CONCLUSION

This paper proposes a new three-dimensional chaotic dynamical system, which is a simple mathematical structure containing two non-linear terms. The fundamental dynamical properties of this chaotic system, the Lyapunov exponents, the Kaplan-Yorke dimension, the bifurcation diagram, the Poincaré map and the topological portraits are studied by numerical simulations. The nonlinear dynamical system designed contains three unstable equilibrium points and a chaotic attractor with complex properties. To demonstrate its effectiveness, an analogue electronic circuit model was implemented using Multisim software. Reach a compromise between a simple chaotic model and complex dynamic behaviour requires ingenuity, adaptability and determination. This quest remains at the forefront of our efforts and has enabled us to unravel the mysteries of chaotic systems while retaining their practicality and relevance to real-world applications. Our future work (new approaches to the control and synchronisation of this system) could lead to concrete applications in the field of secure communications and signal encryption such as image encryption.

REFERENCES

[1] Sciamanna, M., Shore, K. A. (2015). Physics and applications of laser diode chaos. Nature photonics, 9(3), 151-162.

[2] Kapitaniak, M., Czolczynski, K., Perlikowski, P., Stefanski, A., Kapitaniak, T. (2014). Synchronous states of slowly rotating pendula. Physics Reports, 541(1), 1–44. doi: 10.1016/j.physrep.2014.02.008

[3] Escande, D. F. (2016). Contributions of plasma physics to chaos and nonlinear dynamics. Plasma Physics and Controlled Fusion, 58(11), 113001. doi:10.1088/0741-3335/58/11/113001

[4] Jahanshahi, H., Rajagopal, K., Akgul, A., Sari, N. N., Namazi, H., Jafari, S. (2018). Complete analysis and engineering applications of a megastable nonlinear oscillator. International Journal of Non-Linear Mechanics. doi:10.1016/j.ijnonlinmec.2018.08

[5] Heltberg, M. L., Krishna, S., Kadanoff, L. P., Jensen, M. H. (2021). A tale of two rhythms: Locked clocks and chaos in biology. Cell Systems, 12(4), 291-303.

[6] Ataei, M., Chen, S., Yang, Z., Peyghami, M. R. (2021). Theory and applications of financial chaos index. Physica A: Statistical Mechanics and Its Applications, 580, 126160. doi:10.1016/j.physa.2021.126160

[7] Diouf, M., Sene, N. (2020). Analysis of the Financial Chaotic Model with the Fractional Derivative Operator. Complexity, 2020, 1–14. doi:10.1155/2020/9845031

[8] Lorenz, E. N. (1963). Deterministic nonperiodic flow. Journal of atmospheric sciences, 20(2), 130-141.

[9] Lin, H., Wang, C., Yu, F., Xu, C., Hong, Q., Yao, W., Sun, Y. (2021). An Extremely Simple Multiwing Chaotic System: Dynamics Analysis, Encryption Application, and Hardware Implementation. IEEE Transactions on Industrial Electronics, 68(12), 12708–12719. doi:10.1109/tie.2020.3047012.

[10] Javeed, A., Shah, T., Attaullah. (2020). Lightweight secure image encryption scheme based on chaotic differential equation. Chinese Journal of Physics. doi:10.1016/j.cjph.2020.04.008

[11] Talhaoui, M. Z., Wang, X. (2020). A new fractional one-dimensional chaotic map and its application in high-speed Image Encryption. Information Sciences. doi:10.1016/j.ins.2020.10.048
[12] Wang, X., Li, Y., Jin, J. (2020). A new one-dimensional chaotic system with applications in image encryption. Chaos, Solitons and Fractals, 139, 110102. doi:10.1016/j.chaos.2020.110102.
[13] Abdallah, A. A., Farhan, A. K. (2022). A new image encryption algorithm based on multi chaotic system. Iraqi Journal of Science, 324- 337.
[14] Wang, X., Liu, C., Xu, D., Liu, C. (2016). Image encryption scheme using chaos and simulated annealing algorithm. Nonlinear Dynamics, 84(3), 1417–1429. doi:10.1007/s11071-015-2579-y.
[15] Pisarchik, A., Jaimes-Reategui, R., Rodr ´ ´ıguez-Flores, C., Garc´ıa-Lopez, ´ J., Huerta-Cuellar, G., Mart´ın-Pasqu´ın, F. (2021). Secure chaotic communication based on extreme multistability. Journal of the Franklin Institute, 358(4), 2561–2575. doi:10.1016/j.jfranklin.2021.01.013
[16] Jamal, R. K., Kafi, D. A. (2016). Secure communications by chaotic carrier signal using Lorenz model. Iraqi Journal of Physics, 14(30), 51- 63.
[17] Jamal, R. K., Kafi, D. A. (2019). Secure Communication Coupled semiconductor Laser Based on Rossler Chaotic Circuits. IOP Conference Series: Materials Science and Engineering, 571, 012119. doi:10.1088/1757-899x/571/1/012119.
[18] Vangheluwe, H. (2008). Foundations of modelling and simulation of complex systems. Electronic Communications of the EASST, 10.
[19] Posch, H. A., Hoover, W. G. (2004). Large-system phase-space dimensionality loss in stationary heat flows. Physica D: Nonlinear Phenomena, 187(1-4), 281–293. doi:10.1016/j.physd.2003.09.015
[20] Brandstater, A., Swinney, H. L. (1987). Strange attractors in weakly turbulent Couette-Taylor flow. Physical Review A, 35(5), 2207–2220. doi:10.1103/physreva.35.2207.
[21] Lanford, O. E. (1982). The Strange Attractor Theory of Turbulence. Annual Review of Fluid Mechanics, 14(1), 347–364. doi:10.1146/annurev.fl.14.010182.002023.
[22] Dudkowski, D., Jafari, S., Kapitaniak, T., Kuznetsov, N. V., Leonov, G. A., Prasad, A. (2016). Hidden attractors in dynamical systems. Physics Reports, 637, 1–50. doi:10.1016/j.physrep.2016.05.002.
[23] Wolf, A., Swift, J. B., Swinney, H. L., Vastano, J. A. (1985). Determining Lyapunov exponents from a time series. Physica D: Nonlinear Phenomena, 16(3), 285–317. doi:10.1016/0167-2789(85)90011-9.
[24] Kaplan, J. L., Yorke, J. A. (1979). Preturbulence: A regime observed in a fluid flow model of Lorenz. Communications in Mathematical Physics, 67(2), 93–108. doi:10.1007/bf01221359.
[25] Frederickson, P., Kaplan, J. L., Yorke, E. D., Yorke, J. A. (1983). The liapunov dimension of strange attractors. Journal of Differential Equations, 49(2), 185–207. doi:10.1016/0022-0396(83)90011-6.
[26] Alattas, K. A., Mostafaee, J., Alanazi, A. K., Mobayen, S., Vu, M. T., Zhilenkov, A., Abo-Dief, H. M. (2021). Nonsingular terminal sliding mode control based on adaptive barrier function for n th-order perturbed nonlinear systems. Mathematics, 10(1), 43.
[27] H. Poincaré, Mémoire sur les courbes définies par une équation différentielle, Journal de Mathématiques, Série 3, 7, 375-422, 1881 — Série 4, 1, 167-244, 1885.
[28] Rösler, O. E. (1976). An equation for continuous chaos. Physics Letters A, 57(5), 397–398. doi:10.1016/0375-9601(76)90101-8.

[29] G. Chen, T. Ueta, Yet another chaotic attractor, Int. J. Bifurcation Chaos Appl. Sci. Eng., 9(7):1465–1466, 1999.
[30] J. Lu, G. Chen, A new chaotic attractor coined, Int. J. Bifurcation Chaos ¨ Appl. Sci. Eng., 12(3):659–661, 2002.
[31] L.O. Chua, The genesis of Chua's circuit, Archiv fur Elektronik and Ubertragnugstechnik, 46(4):250–257, 1992.
[32] Sprott, J. C. (2000). Simple chaotic systems and circuits. American Journal of Physics, 68(8), 758-763.
[33] Vaidyanathan, S., Azar, A. T. (2016). Adaptive Control and Synchronization of Halvorsen Circulant Chaotic Systems. Studies in Fuzziness and Soft Computing, 225–247. doi : 10.1007/978-3-319-30340-6 10.
[34] THOMAS, R. (1999). DETERMINISTIC CHAOS SEEN IN TERMS OF FEEDBACK CIRCUITS: ANALYSIS, SYNTHESIS, "LABYRINTH CHAOS." International Journal of Bifurcation and Chaos, 09(10), 1889–1905. doi:10.1142/s0218127499001383.
[35] Jia, Q. (2008). Chaos control and synchronization of the Newton–Leipnik chaotic system. Chaos, Solitons and Fractals, 35(4), 814–824. doi:10.1016/j.chaos.2006.05.069.
[36] https://www.analog.com/en/products/ad633.html.
[37] https://www.ti.com/product/TL084A/part-details/TL084ACN.
[38] Tian, K., Grebogi, C., Ren, H.-P. (2021). Chaos Generation With Impulse Control: Application to Non-Chaotic Systems and Circuit Design. IEEE Transactions on Circuits and Systems I: Regular Papers, 68(7), 3012–3022. doi:10.1109/tcsi.2021.3075550.
[39] Abdulaali, R. S., Jamal, R. K. (2022). A comprehensive study and analysis of the chaotic Chua circuit. Iraqi Journal of Science, 63(2), 556-570.
[40] Sambas, A., Vaidyanathan, S., Zhang, X., Koyuncu, I., Bonny, T., Tuna, M., ... Kumam, P. (2022). A novel 3D chaotic system with line equilibrium: multistability, integral sliding mode control, electronic circuit, FPGA implementation and its image encryption. IEEE Access, 10, 68057-68074.
[41] Chua, L. O., Wu, C. W., Huang, A., Guo-Qun Zhong. (1993). A universal circuit for studying and generating chaos. I. Routes to chaos. IEEE Transactions on Circuits and Systems I: Fundamental Theory and Applications, 40(10), 732–744. doi:10.1109/81.246149.
[42] Adıyaman, Y., Emiroglu, S., Uc¸ar, M. K., Yıldız, M. (2020). Dynamical analysis, electronic circuit design and control application of a different chaotic system. Chaos Theory and Applications, 2(1), 10-16.